

Plasmonic resonances of closely-coupled gold nanosphere chains

*Nadine Harris, Matthew D. Arnold, Martin G. Blaber and Michael J. Ford**

The Department of Physics and Advanced Materials and Institute for Nanoscale Technology

RECEIVED DATE

* To whom correspondence should be addressed. Phone: +61 (0) 2 9514 7956. Fax: +61 (0) 2 9514 7553. Email: Mike.Ford@uts.edu.au.

ABSTRACT: The optical properties of an ordered array of gold nanospheres have been calculated using the T-matrix method in the regime where the near-fields of the particles are strongly coupled. The array consists of a 1-dimensional chain of spheres of 15 nm diameter where the number of spheres in the chain and inter-particle spacing is varied. Calculations have been performed with chains up to 150 particles in length and with an inter-particle spacing between 0.5 and 30 nm. Incident light polarized along the axis of the chain (longitudinal) and perpendicular (transverse) to it are considered, and in the latter case for wavevectors along and perpendicular to the chain axis. For fixed chain length the longitudinal plasmon resonance red-shifts, relative to the resonance of an isolated sphere, as the inter-particle spacing is reduced. The shift in the plasmon resonance does not appear to follow an exponential dependence upon gap size for these extended arrays of particles. The peak shift is inversely proportional to the distance, a result that is consistent with the Van der Waals attraction between two spheres at short range which also varies as $1/\text{distance}$. The transverse plasmon resonance shifts in the opposite direction as the inter-particle gap is reduced, this shift is considerably smaller and approaches 500 nm as

the gap tends to zero. Increasing the number of particles in the chain for a fixed gap has a similar effect on the longitudinal and transverse plasmon. In this case, however, the longitudinal plasmon tends towards an asymptotic value with increasing chain length, with the asymptotic value determined by the inter-particle spacing. Here, the approach to the asymptote is exponential with a characteristic length of approximately 2 particles, at small inter-particle spacings. This approach to an asymptote as the chain length becomes infinite has been verified in a finite element calculation with periodic boundary conditions.

KEYWORDS: chain, sphere, plasmon, resonance, near-field

INTRODUCTION: Gold nanoparticles have stimulated considerable research interest owing to their unique optical properties. It is well established that the optical response of an individual gold nanoparticle can be varied by changing the dielectric of the surrounding medium but more dramatically by changing the nanoparticle geometry itself ¹. This has prompted extensive interest in the synthesis and study of the optical response of a wide variety of gold nanoparticle structures such as shells ², rods ³ and stars ⁴ to name a few, where the main aim is to create a particle geometry that provides a very controlled plasmon resonance at the desired wavelength.

Dimers, chains and other arrays of nanoparticles are an alternative method for controlling the position or shape of the plasmon resonance. The optical properties of these arrays can be thought of, at least to a certain degree of approximation, in two regimes. Far-field where the inter-particle gaps are large and there is little overlap between the near-fields of the particles. Diffractive type effects can be seen in this regime when the inter-particle gaps are similar to the wavelength of the incident light and the individual particles have significant scattering cross-sections ⁵⁻⁸. Recently Zou and Schatz ⁶ showed that very large and narrow resonances positioned in the infrared part of the spectrum and giant enhancements in the electromagnetic fields can be produced by large chains of 100 nm diameter silver nanoparticles with very large inter-particle gaps for polarization perpendicular to the chain axis.

In the near-field regime the inter-particle gap is sufficiently small so that the near-fields of the particles are coupled. The plasmon resonance in this regime can be tuned deep into the infrared by decreasing the inter-particle gap and very strong enhancement of the electric field between the particles can be achieved.

A significant amount of research has focused on dimers⁹⁻¹⁸ while studies on long chains (> than 50 particles) have generally focused on their potential applications as substrates for biological sensors that utilize Surface-Enhanced Raman Scattering (SERS)^{6-8, 19} or propagation studies for their potential use as waveguides,^{20, 21} in both cases with inter-particle gaps close to or larger than the wavelength of the incident light. Although Quinten and Kreibig²² have performed T-matrix calculations in the near-contact regime on chains and other arrangements containing 30 silver particles, however their calculations considered the dipole and quadrupole contributions only. An exact expression for the effective permittivity for cubic lattices of spheres has been derived by McKenzie and McPhedran (Nature 265, 128-129 (1977)) based upon the Rayleigh treatment. The authors demonstrate that many orders are required to reproduce the correct divergence of the permittivity as the conducting spheres approach contact. A multiple-scattering method has been applied to clusters containing up to 5 Al nanospheres by Garcia de Abajo (Garcia de Abajo, Phys. Rev. B 60, 6086 (1999)), and a review of light scattering by 2-dimensional periodic arrays of particles and holes has been given by the same author (Garcia de Abajo, Rev. Mod. Phys. 79, 1267 (2007)). More recently, Sainidou and García de Abajo have demonstrated planar metamaterial with large effective permittivity composed of an array of nearly touching particles (Sainidou and García de Abajo, Opt. Express 16, 4499 (2008)). In this work the authors show that these nanoparticle based metamaterials are capable of supporting localized plasmonic modes.

The dimer is an interesting and comparatively well-studied problem²³⁻²⁵. The dipole resonance shifts to longer and longer wavelengths as the spheres approach each other and higher order modes continue to appear at shorter wavelengths. The point of contact is a singularity. As shown recently by Romero *et al.*²⁴ when the contact point is reached an additional mode is possible where charge is transferred between

the two spheres. In practice, other effects such as electron tunneling or necking between the two particles may dominate in the near contact region. Nevertheless, the predicted shift in the resonance with decreasing particle gap has been measured experimentally between gold spheres by Rechberger *et al.*²³ and between gold nanoshells by Lassiter *et al.*²⁶.

It has been proposed that the strong distance-dependence of the resonance wavelength enables dimers to be used as “plasmon rulers”^{9, 27, 28} for measuring distance in objects such as cells. Jain *et al.*⁹ have recently reported a universal scaling behavior for the shift in the resonance of particle dimers and have derived, from optical measurements and calculations, a universal plasmon ruler equation. Lithographical techniques were used to synthesize nanodisc pairs with varying inter-particle gaps. For polarization parallel to the dimer axis the fractional plasmon wavelength shift was observed to decay exponentially with increasing inter-particle gap, with a decay length of 0.2 in units of particle size. Furthermore, the authors found that this decay constant applies to nanoparticles with different sizes or shapes, or particles made from different materials.

In this paper we use computational methods to investigate the optical response of ordered chains of 15 nm diameter gold spheres containing up to 150 particles with small inter-particle gaps. By changing the number of particles in the chain we can investigate the effects of longer range order in the near-field regime and extend the work of Jain *et al.* to long chains of spheres⁹, and that of Zou and Schatz⁶ to the near-field, or near-touching regime. We use the T-matrix method for finite length chains, i.e. without periodic boundary conditions, and finite element methods for infinitely long chains (with periodic boundary conditions).

METHODS: The T-matrix code developed by Mackowski and Mishchenko^{29, 30} was used to calculate the optical extinction of chains of 15 nm diameter gold spheres up to 150 particles in length and with varying inter-particle spacings. Scattering by the chain was calculated for light polarized along the axis of the chain (parallel polarization) and perpendicular to the axis (transverse polarization). The former polarization is only accessible by plane-wave incident light perpendicular to the chain, whereas the

transverse polarization is possible for both a parallel and perpendicular wavevector. Below we will refer to the transverse polarization and wavevector parallel to the chain as ‘end-on’ polarization, and although we have undertaken calculations in this orientation to compare with previous work we do not present the results here. The optical properties of individual gold spheres up to a diameter of about 100 nm are dominated by absorption and one might therefore expect the results presented here for chains of spheres to apply across a similar size range. We have confirmed this in a few representative calculations for various chain lengths and particle sizes, in fact it is the ratio of sphere diameter to interparticle gap that determines the optical properties rather than the absolute value of either quantity.

The dielectric constant of gold in vacuum was taken from Weaver and Frederikse³¹ and no damping contributions from surface scattering have been taken into account as this effect does not become prominent until particle diameter is less than around 5 nm³². The chain length has been varied between 2 and 150 particles and the surface-to-surface inter-particle gap varied between 0.5 and 30 nm.

The T-matrix technique calculates the scattered field from the entire chain as a superposition³³ of the individual fields scattered from each of the spheres within the chain. The individual fields scattered from the spheres are expressed in terms of vector spherical harmonics and with the use of addition theorems a set of equations for the scattered-field expansion coefficients for the entire chain are created²⁹.

In principle, the T-matrix method offers an exact solution to the problem of scattering from arrays of spheres and is a comparatively economic calculation compared with volume discretization methods such as the Discrete Dipole Approximation (DDA). Moreover, the difficulty when using the DDA technique for the present simulations lies in using enough dipoles to adequately resolve the inhomogeneous electric fields between the particles when the inter-particle spacing is small. However, the T-matrix method is not entirely immune from these numerical considerations particularly in the near-contact regime where many orders in the spherical harmonics may be required for the calculation to converge to a reasonable level. Our convergence criteria is defined to be the number of orders required so that the wavelength of the plasmon resonance peak changes less than 1 nm and the variation in magnitude of Q_{ext} is less than 0.001 at the resonance peak.

It is generally accepted that the number of orders required for convergence for an isolated sphere is

$$N = x + 4x^{1/3} + 2 \quad (1)$$

where x is the particle size parameter, $x = \frac{2\pi a}{\lambda}$, a is the sphere radius and λ is the wavelength of the incident light^{29, 34}. Eq (1) gives a lower limit to the number of orders required for convergence. For chains of highly absorbing spheres in the near-contact regime the number of orders will be considerably higher as the singularity at touching is approached. For this reason we have checked the convergence conditions in our calculations carefully for different inter-particle spacings and for different polarizations. The results are shown in Figure 1 for the dimer. The data are plotted as a function of the ratio of inter-particle gap to particle diameter because it is this quantity that scales the scattering properties rather than absolute size of the particle or gap (at least up to a certain particle diameter).

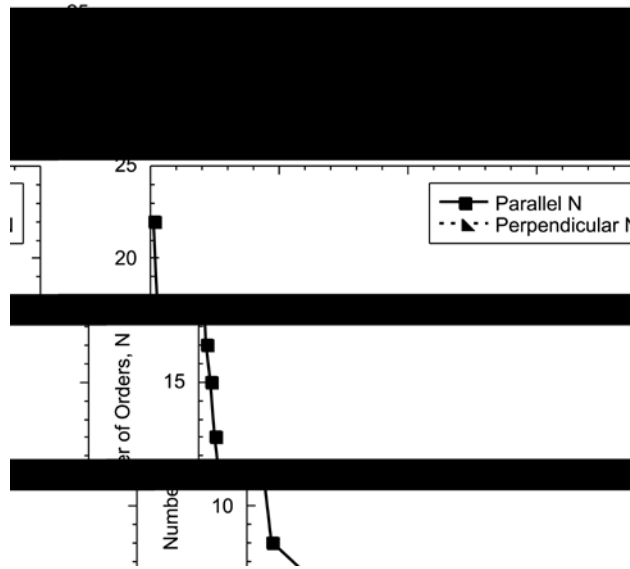


Figure 1. Number of orders of spherical harmonics required for convergence of T-matrix calculations for varying inter-particle gap.

For perpendicular polarization the number of orders remains relatively constant, even at the smallest gaps sizes used here (gap to diameter ratio of 0.03) only 6 orders are required. The number of orders changes around a gap to diameter ratio of 0.3 from 4 to 6 orders because the inter-particle spacing has reduced to the point where more orders are required to resolve the interaction between the electric fields. These results also apply to end-on polarization. For parallel polarization the number of orders increases

rapidly as contact is approached. At a gap of 0.5 nm, corresponding to a ratio of 0.03, 17 orders are required for convergence. Khlebstov *et al.* 25 have reported around 30 orders are required for an inter-particle spacing of 0.15 nm (0.01 ratio) and 40 for an inter-particle spacing of 0.075 nm (0.005 ratio). The dimer convergence criteria reported in Figure 1 have also been tested on chains and calculations which are sufficiently converged for the dimer are converged for a 100 particle chain.

In our calculations we are using the optically determined frequency-dependant dielectric which is effectively a local response. Spatially non-local effects will become important in metallic nanostructures where characteristic feature sizes of the structure are small. These effects in the optical properties of nanospheres have been discussed in some detail in the literature and are commonly described in terms of surface scattering and accounted for by a modified damping term. They are manifest for Au particle sizes below about 5 nm diameter and result in broadening of the plasmon resonance. Recently, a more universal description in terms of a non-local dielectric function and treatment applicable to arbitrarily shaped nanostructures has been given by Garcia de Abajo (F J Garcia de Abajo, *J Phys Chem C*, DOI: 10.1021/jp80734h, 2008). The results indicate that for 20 nm gold dimers non-local effects start to appear at gap spacing of about 0.5 nm and cause a red-shift of the resonance. Hence it is not unreasonable to exclude these effects here as they would only perturb the calculations for the smallest of our gap sizes and not change the overall conclusions.

We have also carried out simulations for an infinite chain using the finite elements package COMSOL 35. A plane-wave source with perpendicular polarization was applied using the scattered-field formalism, and open boundaries were simulated using a cylindrical Perfectly Matched Layer (PML). Longitudinal periodicity was enforced by perfect electric conductors terminating a half-period at the symmetry points. Transverse symmetry was captured with a perfect magnetic conductor termination, reducing the simulation volume by a further factor of two. In addition to reducing computational requirements the high symmetry approach was more numerically stable.

Scattering and absorption cross-sections were determined via surface integrals of the scattered and total fields respectively. Numerical accuracy is generally achieved by adequate numerical sampling of

the fields, especially in strong gradient regions. We set a maximum grid size based on the PML and the meshing algorithm employed by COMSOL ensured finer sampling in the gap where the field is most intense. Field accuracy in this region may benefit from finer sampling but this would have required much greater computational resources. We believe that the sampling employed is sufficiently accurate for the discussions in this paper.

RESULTS AND DISCUSSION: The results of our T-matrix calculations for a 150 particle chain with varying inter-particle spacings are shown in Figure 2 for the parallel and perpendicular polarizations.

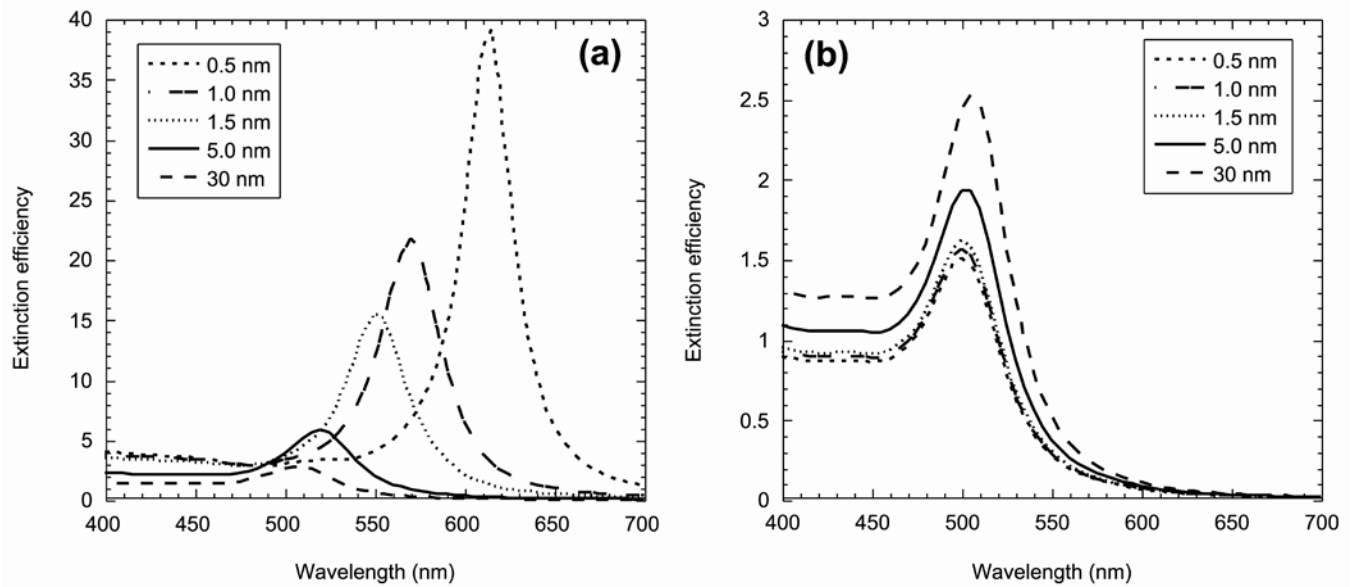


Figure 2. Extinction efficiency for a 150 particle chain with varying inter-particle gaps for (a) parallel polarization and (b) perpendicular polarization.

For the largest gap, 30 nm, both spectra look essentially like an isolated particle with the same plasmon resonance peak for both orientations. As the particles gap decreases the longitudinal and transverse plasmon modes are no longer degenerate and the former shifts to longer wavelengths while the latter shifts to shorter wavelengths. This shift is much more pronounced for the longitudinal mode, the transverse mode approaches a limiting value of 500 nm.

This peak splitting phenomenon agrees with dimer²³ and other chain studies^{21, 22, 36} and qualitative agreement is evident for a 10 particle, 40 nm diameter silver chain with an inter-particle gap of 0.2 nm

(0.005 ratio) modeled by Quinten and Kreibig²², despite having taken only the dipole and quadrupole modes into consideration. Moreover, Brongersma *et al.*³⁷ and others²¹ have reported a $\frac{1}{d^3}$ dependence on the plasmon peak position predicted by the point dipole interaction model, the appropriateness of this dependence to our results will be described later.

The magnitude of Q_{ext} for perpendicular polarization increases as the inter-particle spacing is increased, whereas Q_{ext} increases as the inter-particle spacing is reduced for parallel polarization. This behavior can be understood in terms of a hybridization picture as proposed by Prodan *et al.*³⁸. As the spheres approach, interaction between the plasmon modes of isolated spheres increase and they hybridize into ‘bonding’ and ‘antibonding’ combinations that are shifted to a lower or higher energy respectively relative to the isolated resonance. One might expect more than two hybridized modes given there are more than two particles, although this is not evident in Figure 2. This would suggest that the interaction length of the plasmons on different particles is relatively short, or that the smallest gap we have used here is not small enough to see these higher order modes. At the point of contact Romero *et al.*²⁴ have pointed out that an additional mode is now possible where charge is transferred between the individual particles. Our T-matrix calculations cannot capture this and hence the calculation diverges as the contact point is approached.

For the longitudinal plasmon, Jain *et al.*⁹ have recently demonstrated a universal decay constant for the shift of the plasmon as a function of inter-particle gap. More specifically they plot the shift of the plasmon peak relative to the single particle peak position as a function of the ratio of gap to particle diameter and fit the resulting curve to an exponential. They find a universal scaling constant that applies to different shaped nanoparticles as well as different dielectrics and propose optical measurements of the peak shift as a method of determining distances reliably at the nanoscale.

We have applied the same analysis to our extended chain of 150 particles. The results are shown in Figure 3 where we plot the fractional peak shift ratio, $\Delta\lambda$ versus the ratio of the inter-particle gap to the

particle diameter for a 150 particle chain with inter-particle gaps ranging from 0.5 nm to 30 nm for parallel polarization.

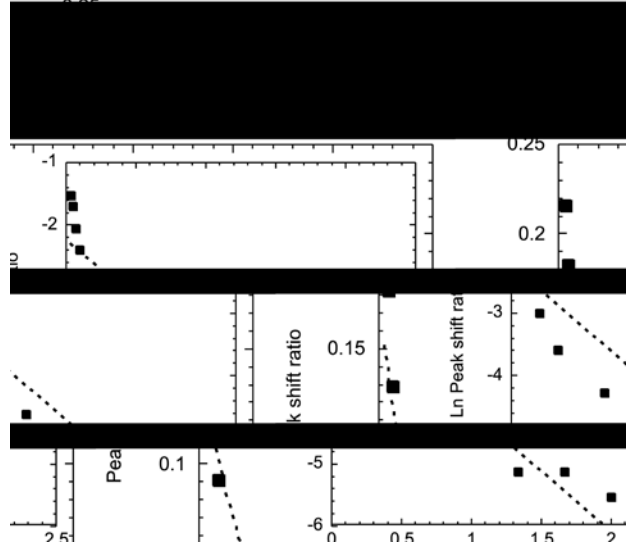


Figure 3. Graph of the ratio of the fractional peak shift ratio versus the ratio of the inter-particle gap to particle diameter for a 150 particle chain. Dotted line is an exponential fit to the calculated points. Inset shows the corresponding natural log plot.

The fractional peak shift ratio is defined as

$$\Delta\lambda = \frac{\lambda_p - \lambda_s}{\lambda_s} \quad (2)$$

where λ_p is the chain plasmon peak position and λ_s is the plasmon resonance for an individual 15 nm diameter gold sphere.

In agreement with Jain *et al.* and previous studies [10, 39](#) the peak shift ratio decays almost exponentially with inter-particle gap. We have fitted an exponential of the form

$$\Delta\lambda = Ae^{-\frac{x}{\tau}} \quad (3)$$

to our calculation, where x is the ratio of inter-particle gap to particle diameter and find the decay constant, τ , to be 0.17. This is close to the result reported by Jain *et al.* However, the quality of this fit is not particularly good with $R^2=0.88$, and the corresponding natural log plot does not yield a straight line. In these calculations we have made sure that the wavelength resolution of our calculations is

sufficient to give reliable values for the peak position at all gap sizes. We have carried out the same analysis for all chain lengths considered here (between 2 and 150 particles) and observe the same behaviour, that is non-exponential scaling of the peak shift.

For gap to diameter ratios greater than about 0.5 the log plot begins to look more linear, fitting an exponential only to this larger gap region gives a decay constant of about 0.40, although even here the quality of the fit is still poor and the error in the fitted decay constant is substantial. Jain *et al.* also neglect calculations at smaller inter-particle gaps from their analysis, but in this case it is because of the difficulty of describing this regime adequately with the DDA technique. Our analysis would suggest that the plasmon peak shift is not exponential in these gap sizes. Moreover, a plot of the transverse and longitudinal plasmon peak positions as a function of the inter-particle spacing (not shown here) are not well represented by the $\frac{1}{d^3}$ dependence reported by Brongersma *et al.*³⁷.

Figure 4 shows a power law fit to the data for the 150 particle chain in figure 3. The corresponding log-log plot is very close to linear with a fitted gradient close to -1 (-0.98). The scaling law for the 150 particle chain would therefore appear to follow an inverse distance dependence. This is perhaps not surprising given that the interaction the van der Waals potential between two spheres at small distance also goes as $1/\text{distance}$. The interaction between the plasmon modes of the two spheres and the van der Waals interaction have a common origin. A similar result is found for chains of other lengths, the log-log plot is remains linear but the gradient differs slightly from -1 , for the bisphere it is -0.89 .

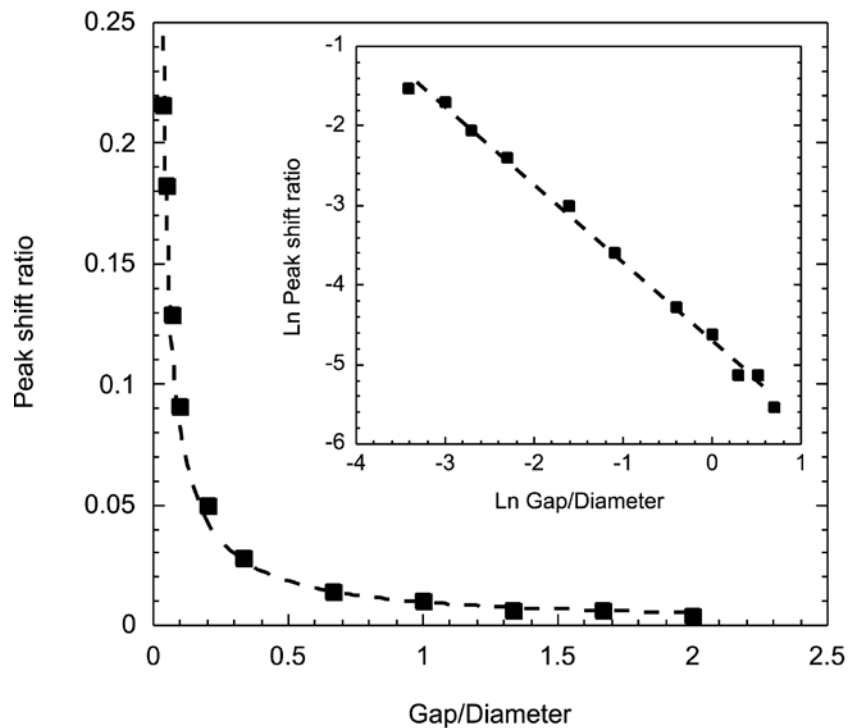


Figure 4. Data of Figure 3 fitted to a power law dependence (dotted line). DInset shows the corresponding natural log-natural log plot .

Figure 4 shows the calculated extinction efficiency spectra this time with a fixed gap size of 0.5 nm for varying length chains for parallel and perpendicular polarization, respectively. The calculation for the infinitely long chain was performed using COMSOL. For clarity only a select number of chains are shown. Note that the Q_{ext} results have been normalized to an individual particle within the chain so that direct comparison can be made with infinite chain calculation.

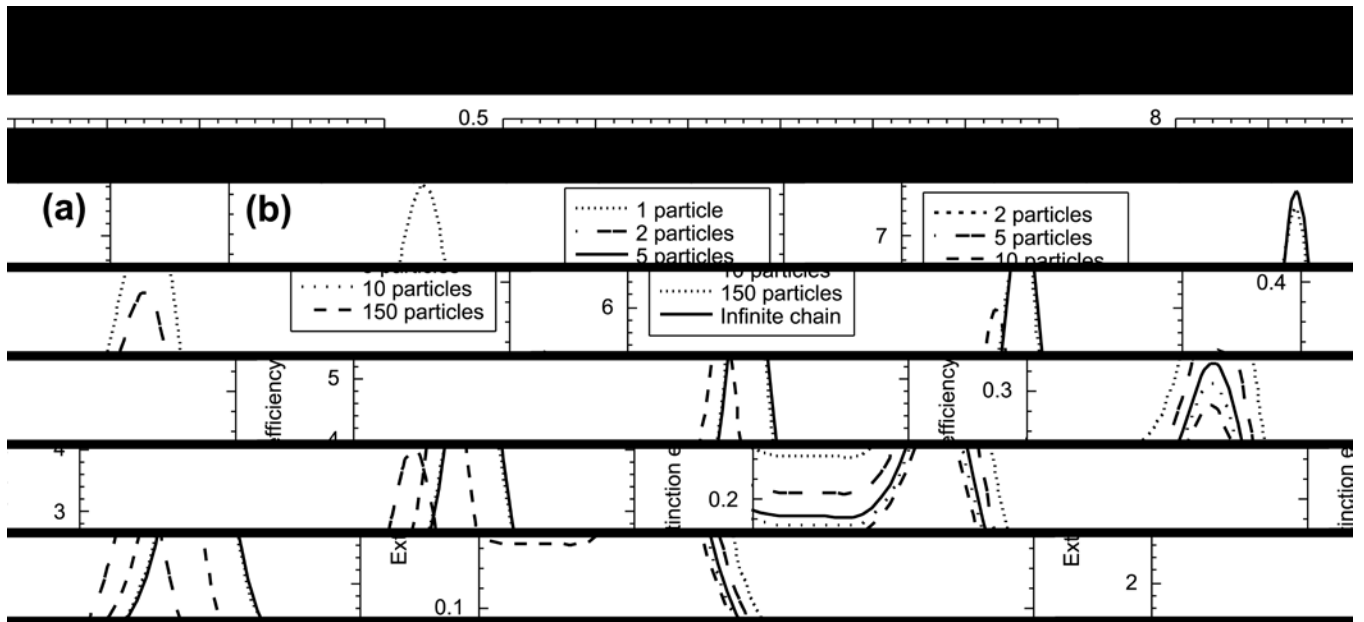


Figure 4. Extinction efficiency normalized per particle for (a) parallel polarization and (b) perpendicular polarization with a 0.5 nm inter-particle spacing.

The overall behavior is similar to the data in Figure 2 where the inter-particle gap was varied for fixed chain length. As the chain length increases the longitudinal plasmon peak (Figure 4(a)) shifts towards longer wavelengths, conversely, the transverse mode shifts towards shorter wavelengths tending towards 500 nm with increasing chain length. However, the longitudinal mode tends towards an asymptotic value with increasing length, in this case for a particle gap of 0.5 nm the peak position for an infinite chain is 614 nm. Even for a 10 particle chain the longitudinal plasmon is already close to its asymptotic value, the result for 150 particle chain is indistinguishable to the infinite length chain.

We have repeated these calculations for different inter-particle gaps, the results are shown in Figure 5 where the fractional peak shift is plotted as a function of chain length.

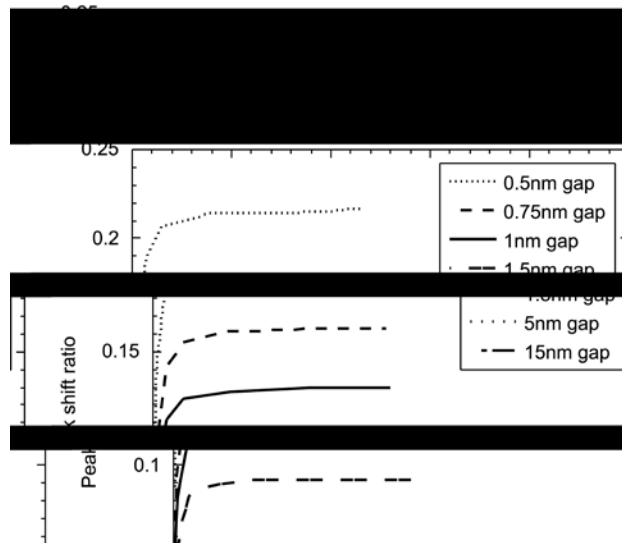


Figure 5. Fractional peak shift ratio for increasing length chains with different inter-particle spacings.

As expected the asymptotic value depends upon the particle gap, with smaller gaps being shifted to longer wavelengths. The 30 nm inter-particle gap results are not shown in Figure 5 because at this spacing the particles are far enough from each other that the response looks like an isolated sphere and the plasmon peak does not shift as the chain length is increased.

The data in Figures 4(a) and 5 indicate the interaction length of the plasmon resonance on the particle chain. The longitudinal plasmon resonance shifts to longer wavelengths as the chain grows because each additional particle adds to the field enhancement between particles along the entire chain. This effect begins to saturate at about 10 particles as evidenced by the fact that the resonance is close to its asymptotic value (Figure 4(a)), or in another words each particle interacts with about its 10 nearest neighbors. These results agree with those of Citrin⁴⁰ who developed a dimensionless model, applicable to any set of chain parameters, to calculate the peak plasmon modes of finite length chains and reported saturation at around 10 particles. Although they differ slightly from the experimental results of Maier *et al.*³⁶ who reported saturation at around 7 particles for chains of 50 nm diameter gold particles with a centre-to-centre spacing of 75 nm.

To make this idea more quantitative we have analyzed the data in Figure 5 in a manner similar to Figure 3. In this case, however an exponential that tends to an asymptote at large chain lengths needs to be fitted to the data:

$$\Delta\lambda = \lambda_o e^{-\frac{m}{x}} \quad (4)$$

where $\Delta\lambda$ is the peak shift ratio defined above, x is the number of chain periods within the chain, m is the characteristic interaction length and λ_o is the asymptotic value for the peak shift.

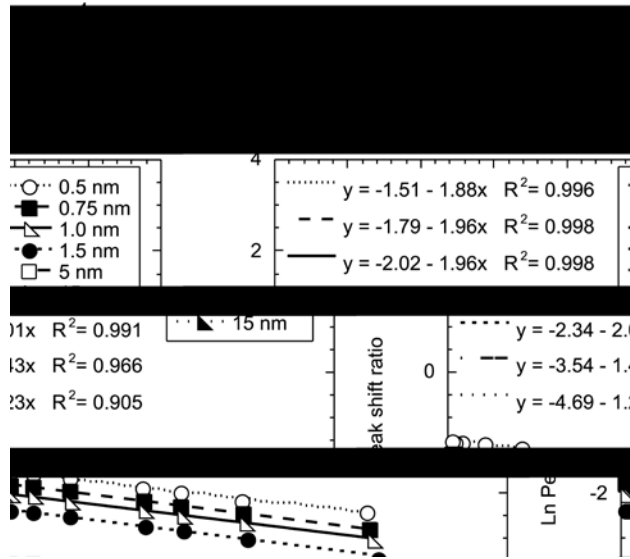


Figure 6. Natural log of fractional peak shift ratio versus the inverse of the number of chain periods.

It is clear from Figure 6 that the exponential form in eq (4) fits the calculated data well for all but the 15 nm gap. The slope of the log plot in Figure 6 is the characteristic interaction length defined in eq (4) in units of the number of chain periods and is almost constant across particle gaps below 5 nm with a value of around 2. This indicates that each particle in the chain has an interaction length of 2 particles, that is, it interacts with its 2 nearest neighbors. This demonstrates that the resonance is localized on the chains. As the inter-particle gap is increased the characteristic interaction length for the 5 nm ($m = 1.43$) and 15 nm ($m = 1.23$) inter-particle gaps reduces and the fit becomes poorer to the point where $m=0$ (not shown) for the 30 nm gap chain indicating that there is little to no coupling between these particles. The y-axis intercepts in Figure 6 give the values of the asymptotic value of the peak position. They agree very well with our finite element calculations for infinite chains.

Figure 7 shows the calculated extinction efficiency per particle with a fixed particle gap of 0.5 nm and varying chain lengths with parallel for perpendicular polarization.

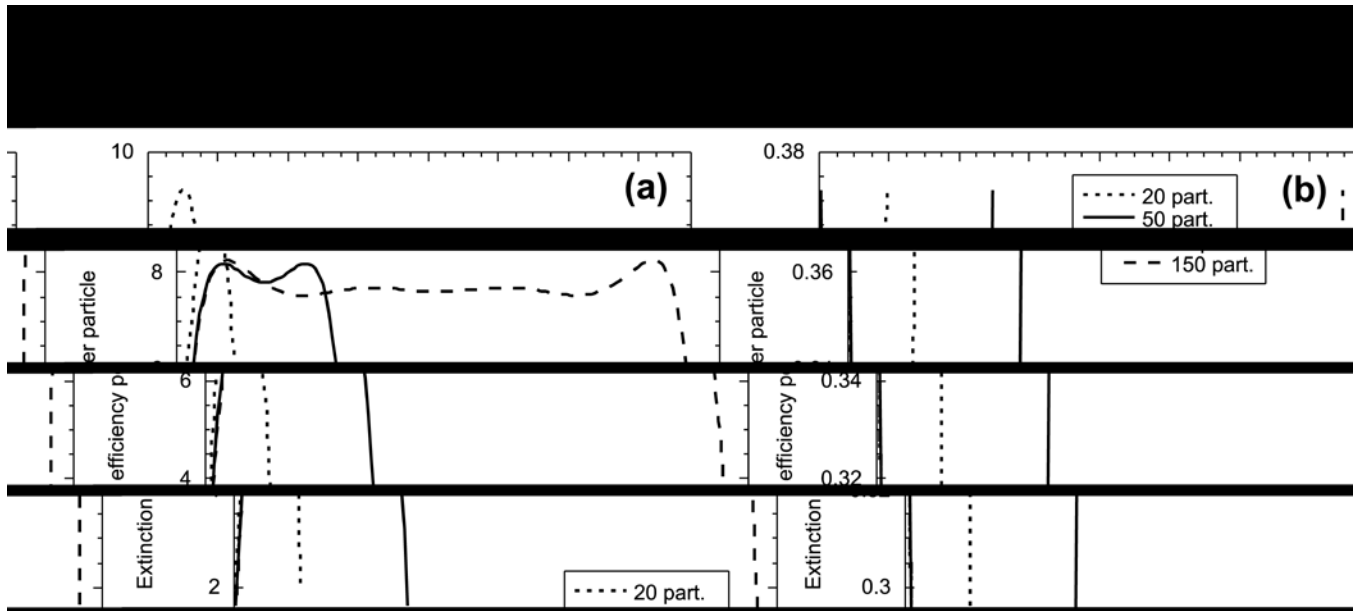


Figure 7. Extinction efficiency per particle for a 0.5 nm inter-particle gap with varying chain lengths and (a) parallel polarization, (b) perpendicular polarization.

The different nature of the longitudinal and transverse resonances is obvious from this figure. Particles at the end of the chain do not contribute significantly to the longitudinal mode. The asymptotic behavior of this mode with increasing chain length is further illustrated in Figure 7 (a), where the extinction distribution along the chain for the 50 and 150 particle chains is qualitatively the same. The rapid increase in extinction efficiency at the ends of the chain gives another indication of the interaction length of the resonance. For the 150 particle chain the extinction reaches its maximum value 5 particles from either end.

The situation is quite different for perpendicular polarization, where the end particles dominate the extinction efficiency. The plots for all three chain lengths are qualitatively the same, and the extinction decreases very rapidly from either end of the chain. The interaction length for the transverse mode is much shorter than the longitudinal mode, or equivalently the plasmon is more localized along the chain. This would seem to be consistent with a TE guided mode in the chain which couples into the far-field

only at the ends of chain. Such modes have recently been described by Sainidou and García de Abajo (Sainidou and García de Abajo, *Opt. Express* 16, 4499 (2008)), for planar arrays of nanoparticles.

From the calculations presented above we know that for inter-particle gaps greater than about 30 nm the near-field coupling between particles is more or less zero and the 15 nm particles within the chain behave in the same way as isolated particles. This is only true for small particles where the scattering efficiency is small. Zou and Schatz⁶ have shown that for larger silver particles (100 nm diameter) increasing the inter-particle gap to the about the same size as the wavelength produces additional structure in the extinction spectrum. Under suitable conditions a very sharp, narrow resonance can be produced in addition to the resonance resulting from plasmon excitation on a single particle. This effect is diffractive in character and hence requires that the individual particles have a reasonable scattering efficiency. The data we have presented above is in the near-field regime where coupling between the particles dominates the extinction and absorption efficiency is the determining factor.

As a final check of our calculations we have performed T-matrix calculations for 150 particle chains with a constant, large particle gap with varying particle diameters. The results are shown in Figure 8.

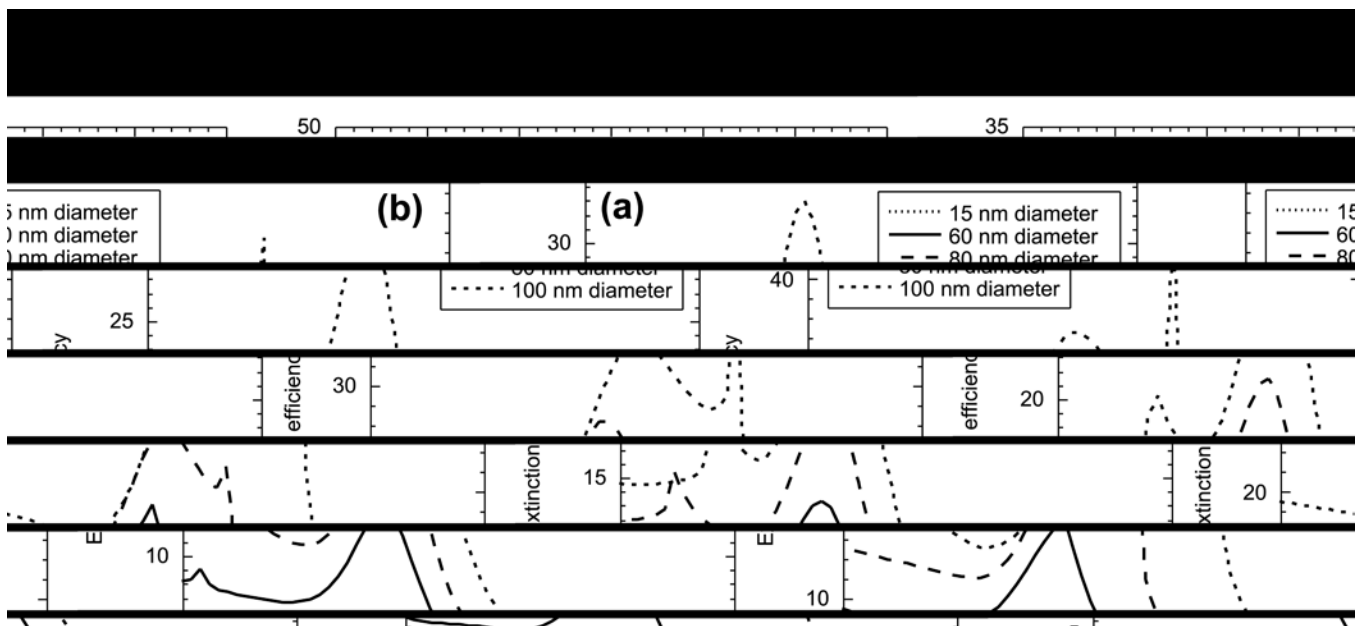


Figure 8. Extinction efficiency for varying diameter particles for a 150 particle chain with (a) an inter-particle spacing of 350 nm and perpendicular polarization, (b) 200 nm gap and end-on polarization.

The present calculations give results which are in agreement with those of Zou and Schatz⁶. A second much narrower resonance begins to appear as the particle diameter increases, becoming apparent for 60 nm particles with perpendicular polarization and at about 80 nm for end-on polarization. This narrow peak shifts in opposite directions for these two polarizations as the particle diameter increases further. For the parallel polarization (not shown) the second sharp peak is absent at particle diameters from 15 to 100 nm. The perpendicular and end-on polarizations are the same, but the incident wavevectors are different, orthogonal to the chain in the former and along the chain in the latter. There is no reason why these two equivalent polarizations should produce the same extinction spectrum for extended chains of particles as the phase of the excitation field is different in the two cases, and certainly Figures 8(a) and (b) demonstrate this. In the near field regime, however, we observe no difference between the two wavevectors for identical polarization even for chains that are longer than the incident wavelength. This is, at first, surprising, but is presumably a consequence of the fact that the interaction length of the resonance is small compared with the wavelength.

CONCLUSION: In summary, we have used the T-matrix technique to model the optical response of varying length chains of 15 nm diameter gold spheres in both the near- and far-field regimes. In the near-field regime the inter-particle gaps were small enough to ensure that the electric fields of the spheres were strongly coupled. Decreasing the inter-particle spacing for a fixed length chain caused the plasmon resonance to split into two separate peaks and blue-shift in the case of transverse polarization and red-shift in the case of perpendicular polarization. However, the peak splitting phenomenon did not follow the $\frac{1}{d^3}$ dependence reported for other chains nor did the red-shifted peak follow an exponential dependence upon gap size that has been associated with dimers. The inverse cube dependence is predicted by a model where the particles are represented by interacting point dipoles (Brongersma *et al.*³⁷). Our calculations suggest that higher order terms cannot be neglected. The number of orders required to reach convergence in our T-matrix calculations supports this conclusion. The exponential

dependence has been predicted in DDA calculations⁹ and could be due to difficulties in describing the rapidly varying electric fields in the gap region using a volume discretization method. The peak shift does, however, follow a power law dependence on the gap distance giving a straight line in log-log plots. This dependence is close to $1/\text{distance}$ for all chain lengths although there is some variation with chain length: the exponent varies from -0.98 to -0.89 for 150 and 2 particle chains respectively. At short distances the Van der Waals interaction (effectively the interaction between plasmon modes) for two spheres is also varies as $1/\text{distance}$.

Increasing the chain length for a constant inter-particle gap caused the longitudinal plasmon peak to exponentially approach an asymptote, the value of which depended upon the inter-particle spacing. For inter-particle gaps below 5 nm the asymptote was reached by around 10 particles and had a characteristic interaction of 2 particles, demonstrating the localized nature of the resonance of the chain within the near-field regime. This behaviour appears to quite general and applicable to all chains with a gap less than 5 nm, that is in the near-field regime.

In the far-field regime 150 particle chains with inter-particle gaps similar to the wavelength of the incident light were modeled. It transpired that the production of a second very sharp, narrow peak was not evident in chains with small particles where the scattering cross-sections are small and only became evident for larger particles with diameters of around 60 nm for perpendicular polarization and around 80 nm for end-on polarization. No second peak was evident for parallel polarization for sphere diameters ranging from 15 to 100 nm.

ACKNOWLEDGMENT: This work was supported by the Australian Research Council (ARC) and the University of Technology, Sydney. Computing facilities were provided by the Australian Centre for Advanced Computing and Communication (ac3) in New South Wales, and the National Facility at the Australian Partnership for Advanced Computing (APAC).

REFERENCES:

1. Schwartzberg, A. M.; Zhang, J. Z. *J. Phys. Chem. C* **2008**, *112*, 10323.
2. Oldenburg, S. J.; Averitt, R. D.; Westcott, S. L.; Halas, N. J. *Chem. Phys. Lett.* **1998**, *288*, 243.
3. Murphy, C. J.; Sau, T. K.; Gole, A. M.; Orendorff, C. J.; Gao, J.; Gou, L.; Hunyadi, S. E.; Li, T. *J. Phys. Chem. B* **2005**, *109*, 13857.
4. Nehl, C. L.; Liao, H.; Hafner, J. H. *Nano Lett.* **2006**, *6*, 683.
5. Zou, S.; Schatz, G. C. *Chem. Phys. Lett.* **2005**, *403*, 62.
6. Zou, S.; Schatz, G. C. *Nanotechnology* **2006**, *17*, 2813.
7. Zou, S.; Janel, N.; Schatz, G. C. *J. Chem. Phys.* **2004**, *120*, 10871.
8. Zou, S.; Schatz, G. C. *J. Chem. Phys.* **2004**, *121*, 12606.
9. Jain, P. K.; Huang, W.; El-Sayed, M. A. *Nano Lett.* **2007**, *7*, 2080.
10. Gunnarsson, L.; Rindzevicius, T.; Prikulis, J.; Kasemo, B.; Kall, M.; Zou, S.; Schatz, G. C. *J. Phys. Chem. B* **2005**, *109*, 1079.
11. Arya, K. *Phys. Rev. B* **2006**, *74*, 195438.
12. Hao, E.; Schatz, G. C. *J. Chem. Phys.* **2004**, *120*, 357.
13. Dahmen, C.; Schmidt, B.; Plessen, G. v. *Nano Lett.* **2007**, *7*, 318.
14. Ruppin, R. *Phys. Rev. B* **1982**, *26*, 3440.
15. Olk, P.; Renger, J.; Wenzel, M. T.; Eng, L. M. *Nano Lett.* **2008**, *8*, 1174.
16. Olk, P.; Renger, J.; Hartling, T.; Wenzel, M. T.; Eng, L. M. *Nano Lett.* **2007**, *7*, 1736.
17. Nordlander, P.; Oubre, C.; Prodan, E.; Li, K.; Stockman, M. I. *Nano Lett.* **2004**, *4*, 899.
18. Mishchenko, M. I.; Mackowski, D. W.; Travis, L. D. *Appl. Opt.* **1995**, *34*, 4589.
19. Yang, Y.; Shi, J.; Tanaka, T.; Nogami, M. *Langmuir* **2007**, *23*, 12042.
20. Zou, S.; Schatz, G. C. *Phys. Rev. B* **2006**, *74*, 125111.
21. Maier, S. A.; Brongersma, M. L.; Kik, P. G.; Atwater, H. A. *Phys. Rev. B* **2002**, *65*, 193408.
22. Quinten, M.; Kreibig, U. *Appl. Opt.* **1993**, *32*, 6173.

23. Rechberger, W.; Hohenau, A.; Leitner, A.; Krenn, J. R.; Lamprecht, B.; Aussenegg, F. R. *Opt. Commun.* **2003**, *220*, 137.
24. Romero, I.; Aizpurua, J.; Bryant, G. W.; Abajo, F. J. G. d. *Opt. Express* **2006**, *14*, 9988.
25. Khlebstov, B.; Melnikov, A.; Zharov, V.; Khlebstov, N. *Nanotechnology* **2006**, *17*, 1437.
26. Lassiter, J. B.; Aizpurua, J.; Hernandez, L. I.; Brandl, D. W.; Romero, I.; Lal, S.; Hafner, J. H.; Norlander, P.; Halas, N. J. *Nano Lett.* **2008**, *8*, 1212.
27. Sonnichsen, C.; Reinhard, B. M.; Liphardt, J.; Alivisatos, A. P. *Nature Biotechnology* **2005**, *23*, 741.
28. Reinhard, B. M.; Siu, M.; Agarwal, H.; Alivisatos, A. P.; Liphardt, J. *Nano Lett.* **2005**, *5*, 2246.
29. Mackowski, D. M. *J. Opt. Soc. Am. A* **1994**, *11*, 2851.
30. Mackowski, D. M.; Mischenko, M. I. *J. Opt. Soc. Am. A* **1996**, *13*, 2266.
31. Weaver, J. H.; Frederikse, H. P. R., *Optical properties of selected elements*. 82 ed.; CRC Press: Boca Raton, FL, 2001.
32. Kreibig, U.; Vollmer, M., *Optical properties of metal clusters*. Springer-Verlag: Berlin Heidelberg, 1995.
33. Borghese, F.; Denti, P.; Saija, R.; Toscano, G.; Sindoni, O. I. *Aerosol Sci. Technol.* **1984**, *3*, 227.
34. Bohren, C. F.; Huffman, D. R., *Absorption and scattering of light by small particles*. Wiley: Weinheim, 2004.
35. <http://www.comsol.com/> <http://www.comsol.com/>
36. Maier, S. A.; Kik, P. G.; Atwater, H. A. *Appl. Phys. Lett.* **2002**, *81*, 1714.
37. Brongersma, M. L.; Hartman, J. W.; Atwater, H. A. *Phys. Rev. B* **2000**, *62*, R16356.
38. Prodan, E.; Radloff, C.; Halas, N. J.; Nordlander, P. *Science* **2003**, *302*, 419.
39. Su, K.-H.; Wei, Q.-H.; Zhang, X.; Mock, J. J.; Smith, D. R.; Schultz, S. *Nano Lett.* **2003**, *3*, 1087.
40. Citrin, D. S. *Nano Lett.* **2005**, *5*, 985.